CRYSTAL GROWTH & DESIGN

Article

pubs.acs.org/crystal

Nucleation Control of Cubic Silicon Carbide on 6H- Substrates

Remigijus Vasiliauskas,*[,†] Maya Marinova,[‡] Philip Hens,[§] Peter Wellmann,[§] Mikael Syväjärvi,[†] and Rositza Yakimova[†]

[†]Department of Physics, Chemistry and Biology, Linköping University, SE-581 83 Linköping, Sweden

[‡]Department of Physics, Aristotle University of Thessaloniki, GR54124 Thessaloniki, Greece

[§]Materials for Electronics and Energy Technology, University Erlangen-Nuremberg, Martensstrasse 7, 91058 Erlangen, Germany

ABSTRACT: The nucleation of cubic (3C) SiC on on-axis 6H-SiC was investigated in the temperature range 1500−1775 °C by the technique of sublimation epitaxy. We have studied two different cases: (i) the initial homoepitaxial growth of 6H-SiC followed by nucleation of 3C-SiC and (ii) nucleation of homoepitaxial 6H-SiC islands. The supersaturation in the growth cell was calculated using the modeled source to substrate temperature difference. We show that, at low temperature and supersaturation, growth of 6H-SiC commences in spiral growth mode, which prepares the surface for 3C-SiC nucleation. Provided the supersaturation is high enough, the 3C-SiC nucleates as two-dimensional islands on terraces of the homoepitaxial 6H-SiC. Detailed structural study indicates that the 3C-SiC began to grow on defect free surfaces. From the experimental and modeling results, we show that the growth parameter window for 3C-SiC is rather narrow. Deviation from it can result in 6H-SiC growth in spiral or 2D-nucleation mode, which suggests the importance of knowledge of supersaturation.

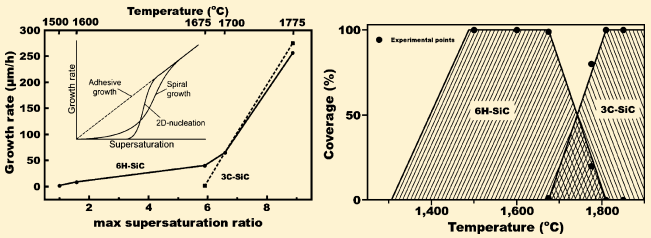

1. INTRODUCTION

The wide band gap semiconductor silicon carbide (SiC) is a material which has the potential to replace silicon in high power and high frequency devices that can operate at high temperatures and within harsh environments, because of superior material characteristics. Silicon carbide exists in different polytypes, among which the most common are 4H-, 6H-, and 3C-SiC. Compared to other polytypes, only 3C-SiC has a cubic structure, the highest saturated electron drift velocity, and a lower density of near interface traps. These advantages make 3C-SiC very desirable for electronic devices. When 3C-SiC is grown on hexagonal substrates such as 4H-SiC or 6H-SiC, it is possible to create heteroepitaxial junctions with two-dimensional electron gas,[1] because of the difference in the band gap energy of these polytypes. This junction would combine the superb properties of SiC, both electrically and physically. The 3C-SiC (111), which forms on 6H-SiC (0001), is also a suitable substrate for graphene growth and may bring new interface properties in such material systems. However, it is still problematic to grow high quality 3C-SiC on hexagonal SiC substrates because of difficulties to control the polytype stability, which is linked to the temperature, substrate, and vapor composition in the growth cell.

The physical vapor transport (PVT) or sublimation process is the most viable technique for fabricating large area SiC crystals, as proven for 6H and 4H-SiC polytypes [e.g., Cree Inc.]. In this work we apply a similar technique to grow 3C-SiC epitaxial layers.[2] Previously we investigated the influence of the substrate surface on the growth of cubic SiC.[2] However, to gain a better fundamental understanding of the 3C-SiC growth, we proceed by analyzing the first stages of its formation on 6H-SiC substrates. The nucleation mechanism and subsequent growth of cubic SiC on nonvicinal 6H-SiC substrates is presented in relation to the vapor supersaturation which is driving the solid phase deposition. It is anticipated that the experimental results combined with modeling in this study will contribute to the knowledge of the growth process and respectively to the improvement of the 3C-material quality.

2. EXPERIMENTAL SECTION

All growth experiments were performed on the Si-face of nominally on-axis (with unintentional off-cut less than 0.5° as specified by the supplier) 6H-SiC (0001) substrates using the sublimation epitaxy technique. The substrates were of 10 × 10 mm^2 size cut from the same wafer. Details of the growth set up and the process can be found elsewhere.[2] In brief, the growth chamber has a close space sublimation geometry implemented in an inductively heated graphite crucible. The temperature is measured by a two color pyrometer on the top of the crucible. The source and the substrate are separated with a graphite spacer, the distance between them is 1 mm, and the growth takes place under vacuum conditions (base pressure 10^{-4}−10^{-5} mbar). A carbon getter (Ta foil) is inserted into the crucible to achieve a higher Si/C ratio. A new source, from the same source wafer, is used for every experiment.

We investigated two different cases: (i) initial homoepitaxial growth of 6H-SiC followed by nucleation of 3C-SiC and (ii) nucleation of homoepitaxial 6H-SiC islands. In the first case, we ramped up temperature to 1500 °C and immediately started cooling down. This is

Received: July 19, 2011
Revised: November 24, 2011
Published: November 28, 2011

followed by an ex-situ examination of the grown sample under an optical microscope. After that the same sample was placed back into the growth chamber and the process was repeated with an increase of the temperature in steps of 50° (or 25°) until 1675 °C was reached. At this temperature 3C-SiC began to nucleate. In order to achieve thick layers, for a comparison with the initial nucleation, the temperature was increased to 1775 °C and kept for 30 min to grow a thick 3C-SiC layer.[2] This was aimed to learn about the growth rate of 3C-SiC and to analyze possible 6H-SiC inclusions. In the second case, the nucleation of homoepitaxial 6H-SiC islands was investigated. Lower Si/C ratio and a temperature ramp up until 1725 °C were applied, after which immediate cool down followed. No growth interrupts were done in this case.

The temperature−time regime is shown in Figure 1. First pumping with a turbomolecular pump was done at room temperature until a pressure of $<10^{-5}$ mbar was achieved. Pumping was maintained through the whole growth process. The temperature ramp up of ∼20 °C/min was used until 1200 °C, where the pyrometer reading started. In the next step, a 5 °C/min temperature ramp up was applied until the growth temperature was reached.

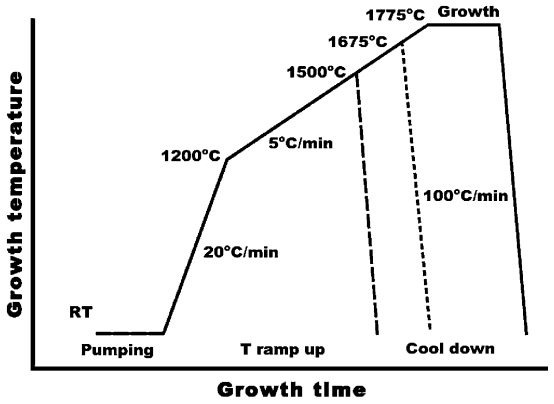

Figure 1. Growth procedure: after pumping, a 20 °C/min temperature ramp up was used to heat up to 1200 °C. The ramp up was changed to 5 °C/min until the desired growth temperature was reached and followed by immediate cool down, or the growth was continued in the standard process.

All temperatures mentioned before are not the ones of the substrate but the ones measured on the top of the crucible, which is colder than the substrate (Figure 2). Differently from most of the other growth techniques, in the sublimation epitaxy, it is not possible to measure the actual temperature of the source and the substrate. In order to know the temperatures of the source and the substrate and the temperature gradient in the growth chamber, we have performed modeling of the temperature field in the crucible at different temperatures measured with the pyrometer (Table 1) using the commercial software Virtual-Reactor (STR) with the SiC-PVT package. For clarification we should mention that the temperature measured on the top (lid) of the crucible is used. The modeled temperatures are used for calculations of the supersaturation ratio, where the temperatures of the source and the substrate are needed.

The numerical modeling of the temperature field is shown in Figure 2. The temperature distribution is shown by different temperature isotherms. A two-dimensional model with rotational symmetry was generated using the actual geometry used for the experimental work. The temperature dependent properties of the different materials were applied to obtain close matching results even for high temperature cases. With a given temperature in the center of the crucible top, as equal to the pyrometer reading in the experimental work, the temperature field was calculated by applying an adjustable power for the simulated induction heating system. The temperature differences at the center of the source and the substrate surfaces were used for the calculation of the supersaturation.

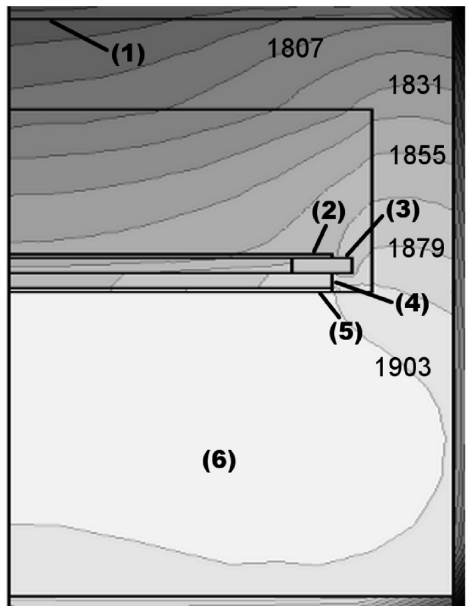

Figure 2. Growth arrangement of sublimation epitaxy for 3C-SiC and calculated temperature distribution in the growth crucible. The temperature on the isotherms is shown (in °C), when the temperature on top of the crucible is 1775 °C. (1) graphite lid; (2) substrate; (3) graphite spacer; (4) SiC source; (5) C getter; (6) bottom part of the crucible.

Table 1. Measured Temperature (T) on the Lid of the Crucible and Modeled Temperature of the Source and the Substrate

pyrometer T (°C)	pyrometer T (K)	substrate T (K)	source T (K)	T diff (K)
1500	1773	1825	1840	15
1600	1873	1931	1947	16
1700	1973	2038	2055	17
1775	2048	2119	2137	18

The surface morphology of the grown material was examined by means of optical microscopy (OM) with Nomarski interference contrast and atomic force microscopy (AFM) in tapping mode. The different SiC polytypes were identified by their different colors in optical transmission microscopy (yellow for 3C and transparent white for 6H) and confirmed using Raman spectroscopy, which was performed by means of an Ar laser (488 nm) with a focused beam (spot size 10 μm) on the sample surface. Microstructural analysis was done by transmission electron microscopy (TEM).

3. RESULTS AND DISCUSSION

It is commonly accepted that the nucleation of cubic SiC requires lower temperature, higher supersaturation, and higher Si/C ratio compared to the conditions for growth of hexagonal SiC polytypes such as 6H and 4H.[3] To nucleate cubic SiC, we exploit these general prerequisites by applying lower temperatures than the ones used for the growth of 6H- and 4H-SiC by the physical vapor transport technique. In the *PVT* process, typically 2200−2400 °C is applied, and for the growth of 3C-SiC by sublimation epitaxy, temperatures below 1900 °C are used.[2] The temperature gradient over the source and the substrate is increased to have higher supersaturation. A tantalum foil was employed to increase the Si/C ratio, since it acts as carbon getter at elevated temperatures. All these conditions enhance the probability of 3C-SiC nucleation.

dx.doi.org/10.1021/cg200929r | *Cryst. Growth Des.* 2012, 12, 197−204

A critical stage in the growth of 3C-SiC is the initial nucleation. In sublimation epitaxy, the formation of nuclei is determined by the temperature and, respectively, the temperature difference between the source and the substrate. As is seen from Table 1, increasing temperature results in larger temperature difference. Therefore, we have studied the initial stage of growth at different temperatures. There was no deposition of cubic SiC at a temperature of 1500 °C, instead homoepitaxial growth commenced by the spiral growth mechanism, forming a 6H-SiC layer. The 3C-SiC started to nucleate as two-dimensional (2D) islands when the temperature was increased to 1675 °C. However, there was no 3C-SiC growth when the Si/C ratio was decreased even though the temperature was further increased, e.g. to 1725 °C. In this case, another type of islands, namely of homoepitaxial 6H-SiC, appeared.

We have identified islands by OM over the whole sample. Later we focused on several islands of each type and confirmed polytype using micro-Raman characterization (Figure 3). For

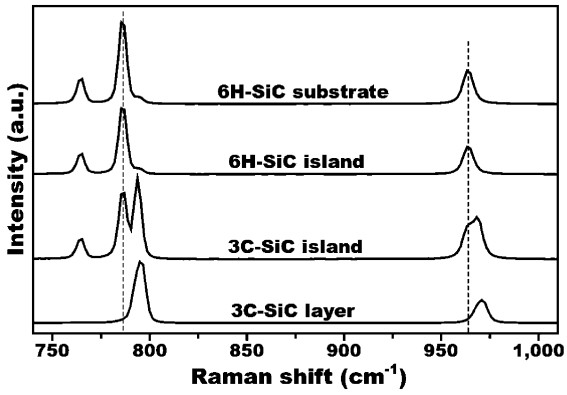

Figure 3. Micro-Raman spectrum of the 6H-SiC substrate, 6H-SiC islands, 3C-SiC island, and thick 3C-SiC layer.

comparison, the 6H-SiC substrate was measured as a reference. From these measurements one can see that the 6H-SiC substrate spectrum has the most intense peaks at 767, 789, and 965 cm^{-1}. The 6H-SiC islands' spectrum is identical to that of the substrate, independently of the growth mechanism of the island (spiral growth or 2D nucleation—discussed later in the text). On the 3C-SiC islands, next to the 6H-SiC peaks, different peaks at 796 cm^{-1} and 972 cm^{-1} appear. The latter peaks are the only ones seen in the thick (125 μm) 3C-SiC layer, confirming the cubic polytype.[4]

3.1. Nucleation of 3C-SiC. To analyze the grown islands in more detail, AFM measurements were applied. A 3C-SiC island grown at 1675 °C is shown in Figure 4a. The island is somewhat roundish with a diameter of 20 μm and a height of 200 nm. The growth steps on the top of the island are 0.25 nm high while the terraces are around 600 nm wide. Also, a few stacking faults can be observed on the top surface of the grown island.

Microstructural investigations of the grown 3C-SiC islands in cross section were performed by TEM. No defects on the 6H-SiC substrate surface were observed from which 3C-SiC would start to nucleate. However, within the 3C-SiC island, extended defects such as stacking faults and 4-fold twins are formed. The latter ones are twinned along the different $\{\bar{1}11\}$ planes. They originate from the 3C/6H-SiC interface and propagate to the surface of the grown layer.[5]

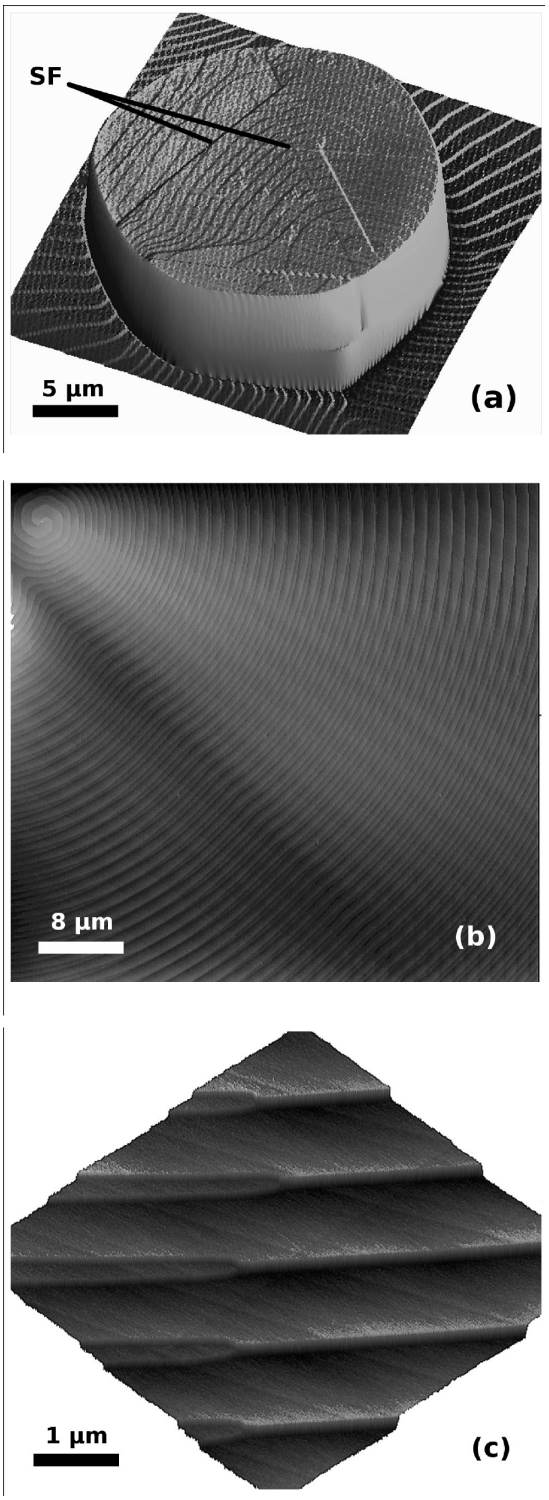

Figure 4. AFM images of sample grown at 1675 °C: (a) the 3C-SiC island (scan size 20 × 20 μm^2); (b) part of two 6H-SiC spirals growing near the 3C-SiC island (scan size 50 × 50 μm^2); (c) magnification of step bunching of the spiral steps (shown in Figure 4b) from 0.75 to 1.5 nm (scan size 5 × 5 μm^2).

Scanning the substrate near 3C-SiC islands revealed that the surrounding 6H-SiC had grown in the spiral growth mode (Figure 4b). This is expected if growth occurs on "atomically flat" (on-axis) SiC substrates.[6] The steps of the spiral are 0.75 nm (half of the 6H-SiC unit cell), and the terrace width is around 0.6−1.3 μm. Steps of half unit cell are typically observed when the

dx.doi.org/10.1021/cg200929r | Cryst. Growth Des. 2012, 12, 197−204

growth is performed at Si rich conditions.[7] During the growth, some of the steps bunched (Figure 4c) into 1.5 nm height steps (full unit cell of 6H-SiC) and the terraces increased in size to more than 1 μm. Incomplete step bunching can be seen on the left side of the image, where half unit cell steps are still present.

In the literature, generally two different scenarios of 3C-SiC nucleation on on-axis hexagonal SiC polytypes (mostly 6H- and 4H-) are described: (i) nucleation induced at substrate defects and (ii) spontaneous nucleation, when high enough supersaturation is reached. In the first case (i), nucleation at defects is of concern when growing hexagonal SiC. Here, the 3C-SiC appears as a parasitic phase. This commonly results in inclusions of 3C-SiC in the grown 6H-SiC (or 4H-SiC) layer, because of the presence of defects, such as scratches, dislocations, or other nonuniformities on the substrate.[8] However, from our TEM characterization, no microdefects were detected on the 6H-SiC substrate from which 3C-SiC could start to nucleate. This indicates a different nucleation mechanism under our growth conditions.

In the other case (ii), typically 3C-SiC layers are targeted for which step and defect free surfaces are employed.[9] Steps and defects on the substrate create more favorable conditions for formation of extended defects such as stacking faults (SFs) and twin boundaries (TBs) in the grown cubic SiC.[10,11] The latter are also known as double positioning boundaries, which propagate from the initial interface to the surface of the grown material and frequently create highly defective areas around them.[12,13] Usually, a step free surface or a surface with low density of steps is achieved by first etching the substrate in situ to remove all scratches and other surface damage. The growth starts at the homoepitaxial 6H-SiC layer, and after that, growth of 3C-SiC takes place. In this case, 3C-SiC starts to nucleate spontaneously in two-dimensional islands when there are no steps or when terraces are wide enough that the supersaturation is sufficient for 2D-nucleation to occur.

Our study is aimed at 3C-SiC growth on 6H-SiC substrates, which falls into the frame of the second case, however, with some peculiarities which are characteristic of the sublimation growth technique. At low temperatures, before supersaturated vapor is established above the substrate, there is a certain sublimation of the substrate (<1 μm) during the temperature ramp-up, which makes the surface smoother. This process helps to avoid nucleation on a rough surface, which would result in the growth of low quality material (higher density of TBs). However, at the same time, screw dislocations intersecting the substrate surface are revealed. Hence, the growth of homoepitaxial 6H-SiC begins from screw dislocations in the spiral growth mode, which takes place already at about 1500 °C. During this stage, eventual scratches left from an imperfect polishing are overgrown. With increasing growth temperature, the terrace width increases. However, as the 6H-SiC grows by a spiral mechanism, it is impossible to attain a step free surface. Typical widths of the terraces are from 0.6 to 1.3 μm before the 3C-SiC nucleates.

In the 1675−1700 °C temperature interval, the supersaturation is high enough and the initial 3C-SiC nucleation occurs via two-dimensional islands on the 6H-SiC terraces. This observation is different from what is commonly reported: that the 3C-SiC starts to grow on perfectly on-axis facets directly on the substrate.[14] The 6H-SiC growing in the spiral mode provides steps instead of large terraces, thus limiting the growth of 3C-SiC, and as previously mentioned, it could result in more defects in the layer. Nevertheless, it is possible to control the size of the terraces by using a different temperature ramp up and by this to obtain larger 3C-SiC domains and lower density of TBs.[15] We apply a 5 °C/min ramp up for all growth experiments, which gives large terraces, and a quite thick (20−40 μm) homoepitaxial 6H-SiC layer is grown before the growth of 3C-SiC starts. This process enables us to achieve higher quality material (lower TB density) growth over large areas, compared, e.g., to small area growth proposed by other researchers.[9] The 3C-SiC islands expand normally and laterally, overgrowing to a large extent the 6H-SiC layer. However, at the same time, 6H-SiC is also growing and competing with the growth of cubic SiC.

To better understand why 6H-SiC is not fully overgrown, we have done AFM studies of 6H-SiC inclusions in samples with 125 μm thick epilayers grown at 1775 °C for 30 min with a growth rate of 250 μm/h. Here the coverage of the substrate by 3C-SiC is ∼90%. In this case the homoepitaxial 6H-SiC grows also by the spiral mechanism. The main difference in the 6H-SiC inclusions in the 3C-SiC layer is the height of all spiral steps (1.5 nm) and the terrace width (300−600 nm), compared to the case of the 6H-SiC spirals growing before the 3C-SiC starts to nucleate, where the step height is predominantly 0.75 nm and the terrace width is 600−1300 nm. Most probably, the smaller terraces result in lower supersaturation and are not preferable sites for 3C-SiC nucleation. This result suggests the importance of terrace width and, respectively, supersaturation for the survival of the 3C-SiC polytype.

3.2. Nucleation of 6H-SiC Islands. It is worth noting that slightly changed growth conditions can result in homoepitaxial 2D-nucleation of 6H-SiC to appear instead of 3C-SiC. In our case it was obtained by an increasing temperature to 1725 °C and a slight decrease of the Si/C ratio by using the same Ta foil for several experiments, with all other conditions being the same. Two different 6H-SiC islands were identified. One type of islands grew by a spiral growth mode (Figure 5a). These are growing mainly near the edges of the growth area. The lower part of the island is hexagonal, and the top has a truncated conelike shape. The diameter at the bottom is larger than that of the top part. These islands are much higher than the 3C-SiC ones described earlier. The parameters of all islands are summarized in Table 2.

These homoepitaxial 6H-SiC islands are different from the 6H-SiC spirals described earlier, as the first ones do not complete a whole layer but are localized. A spiral on the top of the island is suggesting that it has started from a screw dislocation. This type of growth is usually achieved when growing 6H-SiC on on-axis substrates. The spiral growth originates from screw dislocations, and much lower supersaturation is needed to start the growth.[6] Such a growth mode is not unexpected because the substrate contains screw dislocations in the range 10^3−10^4 cm^{-2}.

The other type of the homoepitaxial 6H-SiC islands is more unusual, because there were no growth related spirals observed (Figure 5b). The islands have irregular shape, and on the top there are hexagonal features indicating the two-dimensional growth nature. The diameter of the island is similar to that of the 3C-SiC islands, but the 6H-SiC ones are much higher even though they are smaller than the ones grown by the spiral growth mechanism. The density of these 6H-SiC islands is around 2−3 times lower than that of the 3C-SiC grown at 1675 °C, and the distribution is uniform over the whole sample. These islands could not be formed due to masking, for example, by some particles, as the growing surface is facing downward and there are no scratches on the top of the island, even though they are present on the initial surface. Most probably, these islands start to grow on an atomically flat surface after coalescence of several nuclei. The appearance of this kind of 6H-SiC islands could be due to several reasons. One is

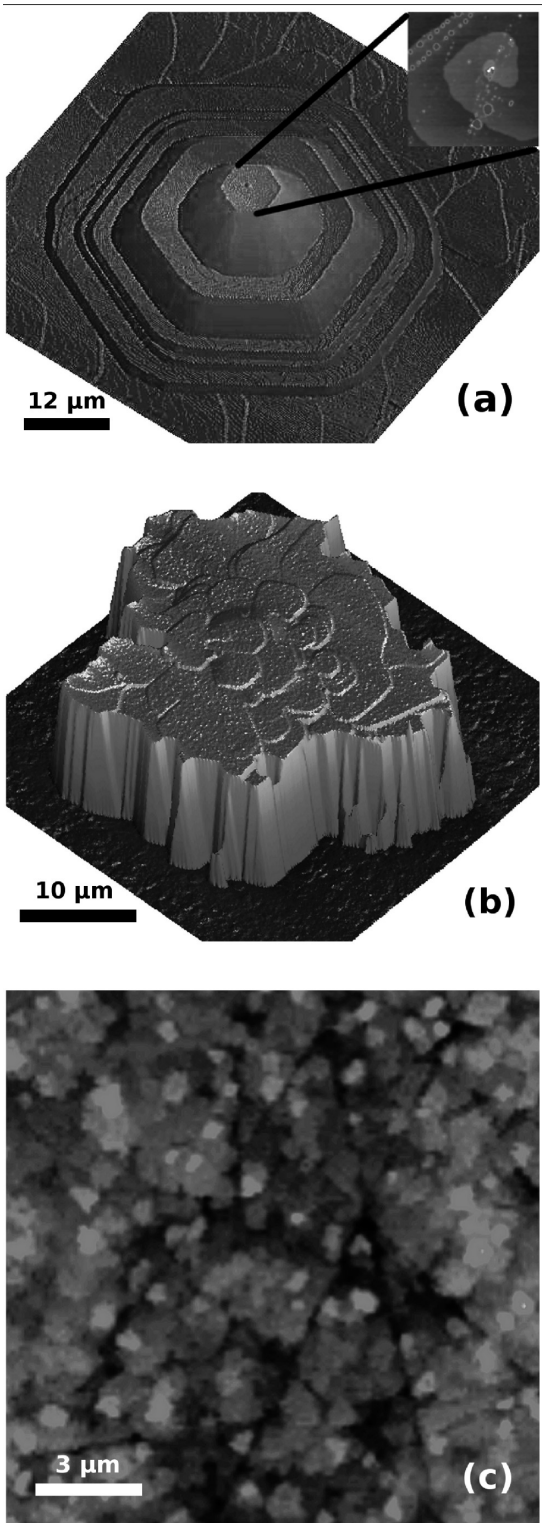

Figure 5. AFM image of sample grown at 1725 °C: (a) The 6H-SiC hillock grown by the spiral growth mechanism (scan area 60 × 60 μm^2). Inset: Spiral on the top of the hillock. (b) Irregularly shaped 6H-SiC 2D island (scan area 35 × 35 μm^2). Hexagonal features are observed on top of the island. (c) Almost no growth near the 6H-SiC islands without spiral. Polishing scratches on the substrate and some small islands are observed (scan size 15 × 15 μm). Depth of scratches 2–9 nm.

nonactivation of spirals;[16] another is that the screw dislocation density was rather low. Typically, screw dislocations distribution is very nonuniform in the substrates. Besides that, we could not detect any defects either on the substrate from which 6H-SiC islands would start to grow or in the grown island when analyzing by cross-sectional TEM. To our knowledge, such homoepitaxial 2D-nucleated 6H-SiC islands are observed experimentally for the first time.

Interestingly, near the 6H-SiC islands without spirals, there is almost no growth on the substrate. One can still see scratches which are left from imperfect polishing of the substrate (Figure 5c). The only growth observed is near the scratches as small islands (2–4 nm in height and 300–600 nm in width) of 6H-SiC. The small island radius (r = 150–300 nm) is much larger than the critical radius (r_{crit} = 5.4 nm). The critical radius is given by $r_{crit} = \sigma\Omega/\Delta\mu$, where σ is the surface free energy (1767 erg/cm^2), Ω is the molecular volume (2.07×10^{-23} cm^3), and $\Delta\mu$ is the driving force, $\Delta\mu = \ln(P/P_0)kT$, where P_0 is the equilibrium vapor pressure and P is the actual vapor pressure. Thus, if the growth process would be continued, the islands would not disappear but expand and coalesce, forming a large 6H-SiC island or a layer.

The higher size of the 6H-SiC spiral grown island (Table 2) indicates that it has nucleated earlier and/or the growth rate was higher than those for the other types of islands. The other types of islands are much smaller, as they have nucleated later, when supersaturation was higher. Initially, the 3C-SiC islands are the smallest of all island types, because they nucleated late. Additionally, together with the 3C-SiC islands, there is homoepitaxial 6H-SiC, which is also growing around the island. For this reason, the exact height of the 3C-SiC island is hard to determine.

The formation of homoepitaxial 6H-SiC islands under overall process conditions for 3C-SiC growth demonstrates that the window of parameters for growth of cubic SiC is rather narrow. Therefore, parameters such as temperature, temperature gradient, Si/C ratio, etc. have to be controlled carefully in order to grow 3C-SiC with a low density of 6H-SiC inclusions.

3.3. Evaluation of the Nucleation Driving Force. For a deeper understanding of the conditions for controlled nucleation of cubic SiC, we have evaluated the supersaturation ratio, $\alpha = n_s/n_{s0}$, where n_s is the number of adsorbed atoms per unit area on the surface and n_{s0} is the adatom concentration at equilibrium.

Our growth experiments were performed on on-axis SiC substrates, which ideally should not contain any steps. However, there is always some small off-cut angle (<0.5°, as specified by the supplier), and what is more important, there is spiral growth of homoepitaxial 6H-SiC which creates steps. On a microscale, the spiral steps far from the spiral center are very similar to the ones in step flow mode. Therefore, for the calculations of the supersaturation ratio, we discuss growth of SiC in frames of a simple diffusion model based on the Burton–Cabrera–Frank theory,[17] where equal steps of height h and terraces of length λ_0 are considered (Figure 6a). The adatoms on the surface can migrate until they reach the kink of a step and are incorporated into the growing material or desorbed from the surface. All adatoms reaching the kinks are incorporated; therefore, the supersaturation ratio α at kinks is equal to one.

A similar approach for calculations of supersaturation ratio during the growth of hexagonal SiC by chemical vapor deposition (CVD) in the step flow growth mode has been used by Kimoto et al.[18] However, the supersaturation ratio has not been calculated for the sublimation epitaxy growth technique. One of the reasons for this is that it is not possible to know the exact temperature of the substrate and the source at the growth

Table 2. Morphological Parameters of the Islands

island type	growth temp (°C)	height (μm)	diameter (μm)	features on the top of island
3C-SiC islands	1675	0.2−0.25	20−25	0.25 nm height steps. Stacking faults.
6H-SiC islands with spirals	1725	2−4	35−40 (bottom) 6−7 (top)	0.75 nm steps. Spiral.
6H-SiC islands without spirals	1725	1.0−1.5	27−29	Hexagonal features 3.5 μm in diameter and 7 nm in height.

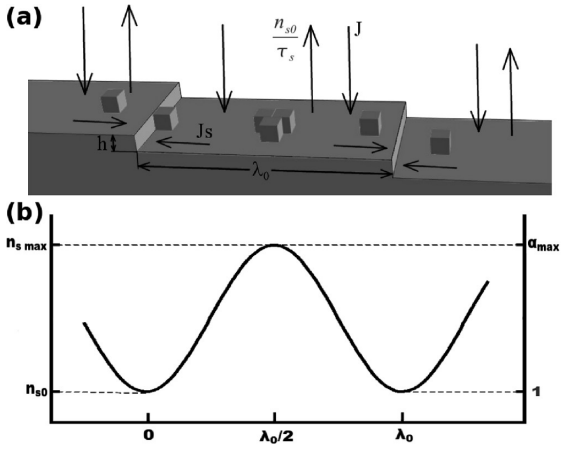

Figure 6. (a) Schematic illustration of a surface diffusion model; J is the arriving flux of the atoms from the source. (b) Distribution of adatom concentration and supersaturation ratio on a stepped surface.

conditions, and modeling with the actual geometry of the growth cell is needed.

The maximum supersaturation which is in the middle of a terrace (Figure 6b) can be expressed by[18]

$$\alpha_{max} = 1 + \frac{\lambda_0 n_0 R}{2\lambda_s h}\frac{\tau_s}{n_{s0}}\tanh\left(\frac{\lambda_0}{4\lambda_s}\right) \quad (1)$$

where λ_0 is the terrace length, λ_s is the surface diffusion length, $n_0 = 1/a^2$ is the density of adsorption sites on the surface (1.06×10^{15} cm^{-2}), a is the lattice constant, R is the growth rate, h is the step height (0.25 nm), and n_{s0}/τ_s is the desorption flux. The terrace length, surface diffusion length, and growth rate depend on experimental conditions, and other parameters are constants for the material.

Using the Hertz−Knutsen equation from the kinetic theory of gases and the equilibrium vapor pressure P_0 of silicon, we can calculate the desorption flux from the SiC substrate:

$$\frac{n_{s0}}{\tau_s} = \frac{P_0}{\sqrt{2\pi m k_b T}} \quad (2)$$

where m is the mass of the species, k_b is the Boltzmann constant, T is the substrate temperature, and P_0 is the equilibrium pressure of the vapor above the SiC substrate.[19] To calculate the desorption flux, the vapor pressure of silicon over SiC was used, because silicon has the highest vapor pressure in the growth area at the temperatures used in this study and the lack of silicon causes carbonization of the source, resulting in a rapid drop of the growth rate.[20]

Equation 2 was used to calculate the incoming flux of the atoms to the substrate surface (Figure 7), which is the desorption flux from the source. There is no deposition on the walls of the crucible, because of the small distance between the source and the substrate. It is assumed that all flux leaving the source reaches the substrate and contributes to the growth.

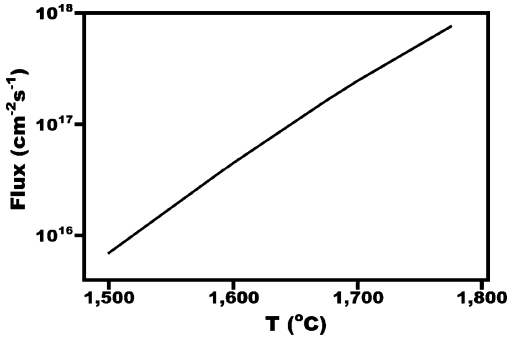

Figure 7. Calculated atom flux to the substrate as a function of temperature.

When the maximum supersaturation ratio reaches a critical value called critical supersaturation, α_{crit}, two-dimensional nucleation of disk shaped nuclei commences. This can be expressed by the following:

$$\alpha_{crit} = \exp\left(\frac{\pi h \sigma^2 \Omega}{(65 - \ln(10^{12}))k_b{}^2 T^2}\right) \quad (3)$$

where σ is the surface free energy of the 6H-SiC substrate (1767 erg cm^{-2} (ref 21)) and Ω is the volume of the Si−C pair (2.07×10^{-23} cm^3). The α_{crit} can be calculated from the growth parameters when the 3C-SiC started to nucleate.

At critical conditions $\alpha_{crit} = \alpha_{max}$. Using this relation, we can rewrite eq 1, and knowing α_{crit}, we can calculate surface diffusion length λ_s at 1675 °C:

$$\frac{\lambda_0}{4\lambda_s}\tanh\frac{\lambda_0}{4\lambda_s} = \frac{(\alpha_{crit} - 1)h}{2n_0 R}\frac{n_{s0}}{\tau_s} \quad (4)$$

The calculated surface diffusion length ($\lambda_s = 3.7 \times 10^{-6}$ cm) at 1675 °C is very close to the one determined by ref 18. For this reason, for calculations of maximum supersaturation ratio at other temperatures, λ_s was taken from ref 18 after recalculating with the surface free energy of 6H-SiC (1767 erg cm^{-2}).

The terrace size of 6H-SiC for the calculation of the maximum supersaturation ratio was taken from the experimental data shown in Figure 8. The terrace size increases exponentially

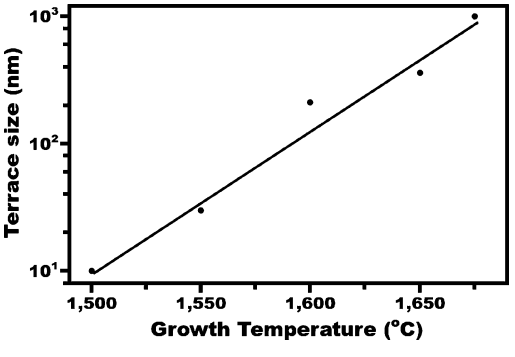

Figure 8. Step terrace size dependence on temperature.

dx.doi.org/10.1021/cg200929r | Cryst. Growth Des. 2012, 12, 197−204

with the temperature, reaching more than 1 μm at 1675 °C. At this point, 3C-SiC may be formed and the terraces of 6H-SiC are not increasing in size because they are overgrown.

The sublimation−recondensation process has a big potential of growing 3C-SiC with a high growth rate, which is very important for a commercially viable growth process. Hence, it is important to calculate the supersaturation ratio and understand its relation with the experimentally known growth rate for a particular growth setup.

In order to find the dependence of the growth rate on the supersaturation (Figure 9), we used the experimental growth

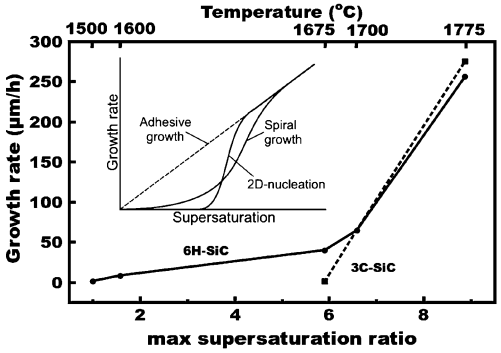

Figure 9. Growth rates of 6H-SiC growing by spirals and 3C-SiC growing by 2D-nucleation growth mode as a function of supersaturation ratio. The top scale shows at which temperature supersaturation was calculated. In the inset is shown the theoretical dependence of growth rate on supersaturation.[17]

rate of 6H-SiC for high temperatures (1675−1775 °C)[20] and the extrapolated ones for the low temperatures (1500−1675 °C). However, there are only two points where the growth rate of 3C-SiC was possible to determine. One is the nucleation point, where the growth rate is near zero, and another point is at normal growth at 1775 °C. By connecting these points, we can see that the tendency is close to the one for 6H-SiC in this supersaturation region.

The obtained growth rate dependence on the supersaturation ratio (Figure 9) is very similar to the initial course of the theoretical dependence (Figure 9 inset).[17] When a temperature of 1500 °C is reached and the supersaturation ratio is just over unity, the homoepitaxial growth of 6H-SiC starts from dislocations by the spiral growth mechanism. This supersaturation is not enough for 2D-nucleation of 3C-SiC to occur. Further increase of the supersaturation ratio was achieved by increasing temperature and because terrace size increases, as well. When the maximum supersaturation ratio becomes equal to the critical supersaturation ratio (at around 1675 °C), the 2D-nucleation of 3C-SiC begins. The generation of 2D-nuclei increases exponentially with the supersaturation ratio and 3C-SiC overgrows most of the 6H-SiC spirals. However, the difference in the growth rate of 3C- and 6H-SiC is small and if the supersaturation becomes lower at some areas, for instance, because of the smaller terrace width on some spirals, 6H-SiC growth will predominate. This can explain why increasing the growth temperature (resulting in higher supersaturation) to more than 1800 °C helps to achieve nearly 100% overgrowth of the substrate by 3C-SiC (results not shown here). At higher growth temperatures, a higher growth rate is achieved (e.g., 400−800 μm/h); however, the quality of the grown 3C is low. Such a high growth rate can be achieved because of the flux of the arriving species, and more importantly, the difference between incoming species and desorbing ones increases exponentially with the temperature (Figure 7). However, the nucleation and the growth rate of 3C-SiC are also dependent on other conditions, such as Si/C ratio, temperature distribution, etc., which can cause fewer nuclei and lower growth rate at some locations of the sample. Because of that, it is difficult to achieve full coverage of the substrate by 3C-SiC.

In Figure 10 we summarize 6H-SiC and 3C-SiC phase occurrence vs process temperature. Clearly, 3C-SiC growth is

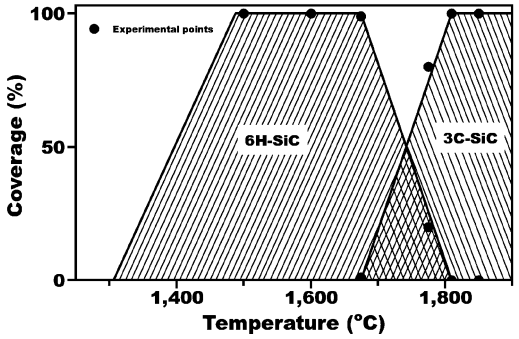

Figure 10. Coverage of the substrate by different polytypes of SiC at different temperatures.

preceded by that of homoepitaxially grown 6H-SiC spiral terraces without facets, and the process requires much higher supersaturation for 3C-SiC to nucleate and maintain stable growth. The latter observation is in agreement with previous works,[3] while the former one is for the first time reported here. This appears to be in contrast with the common belief that 3C-SiC formation is the first one to happen in SiC sublimation growth.[22]

4. CONCLUSIONS

The nucleation and growth of cubic silicon carbide by sublimation epitaxy on nominally on-axis 6H-SiC substrates is studied. It is shown that the nucleation of 3C-SiC does not start from substrate defects. Instead, it occurs on terraces created by the homoepitaxial 6H-SiC growing in spiral mode, which begins much earlier than the 3C-SiC growth. Control of the homoepitaxial layer growth may be a key element in fabricating 3C-SiC with a low density of 6H-SiC inclusions and twin boundaries. A number of process parameters, such as temperature, temperature gradient, and Si/C ratio, have a substantial influence on the growth. Thus, only a small window of parameters is available for the growth of good quality 3C-SiC. From experiments and calculations of the supersaturation, we can conclude that at low temperature (respectively supersaturation) the growth of the 6H-SiC polytype is preferred. At higher supersaturation, 3C-SiC starts to nucleate and overgrows the 6H-SiC layer to a large extent. It was found that the overall 3C-SiC evolution by sublimation epitaxy in this study is close to the theoretically predicted one. That points to the ability of developing well controlled operational conditions for growth of device quality cubic SiC.

■ AUTHOR INFORMATION

Corresponding Author

*Telephone: +46-13-281704. Fax: +46-13-137568. E-mail: remis@ifm.liu.se.

■ ACKNOWLEDGMENTS

The authors acknowledge E. K. Polychroniadis for the help with TEM measurements. This work was supported by the Swedish Research Council (Contract No. 1220100821) and FP6 Marie Curie Action - Research and Training Network - MANSiC - Contract No. 035735. Mikael Syväjärvi acknowledges support from Ångpanneföreningen Research Foundation and Swedish Energy Agency. Peter Wellmann and Philip Hens acknowledge support from Bundesministerium für Bildung und Forschung (BMBF) under contract number 03SF0393.

■ REFERENCES

(1) Polyakov, V. M.; Schweirz, F. *J. Appl. Phys.* **2005**, *98*, 023709.
(2) Vasiliauskas, R.; Marinova, M.; Syväjärvi, M.; Liljedahl, R.; Zoulis, G.; Lorenzzi, J.; Ferro, G.; Juillaguet, S.; Camassel, J.; Polychroniadis, E. K.; Yakimova, R. *J. Cryst. Growth* **2011**, *324*, 7−14.
(3) Fissel, A. *J. Cryst. Growth* **2000**, *212*, 438.
(4) Nakashima, S.; Harima, H. *Phys. Status Solidi A* **1997**, *162*, 39.
(5) Vasiliauskas, R.; Marinova, M.; Syväjärvi, M.; Mantzari, A.; Andreadou, A.; Lorenzzi, J.; Ferro, G.; Polychroniadis, E. K.; Yakimova, R. *Mater. Sci. Forum* **2010**, *645−648*, 175.
(6) Byrappa, K.; Ohachi, T. *Crystal growth technology*; Springer: Norwich, NY, William Andrew: Berlin, 2003.
(7) Matsunami, H.; Kimoto, T. *Mater. Sci. Eng.* **1997**, *R20*, 125.
(8) Powell, J. A.; Petit, J. B.; Edgar, J. H.; Jenkins, I. G.; Matus, L. G.; Yang, J. W.; Pirouz, P.; Choyke, W. J.; Clemen, L.; Yoganathan, M. *Appl. Phys. Lett.* **1991**, *59*, 333.
(9) Powell, J. A.; Neudeck, P. G.; Trunek, A. J.; Beheim, G. M.; Matus, L. G.; Hoffman, R. W. Jr.; Keys, L. J. *Appl. Phys. Lett.* **2000**, *77*, 1449.
(10) Nishino, K.; Kimoto, T.; Matsunami, H. *Jpn. J. Appl. Phys.* **1997**, *36*, 5202−5207.
(11) Chien, F. R.; Nutt, S. R.; Yoo, W. S.; Kimoto, T.; Matsunami, H. *J. Cryst. Growth* **1994**, *137*, 175−180.
(12) Kong, H. S.; Jiang, B. L.; Glass, J. T.; More, K. L.; Rozganyi, G. A. *J. Appl. Phys.* **1988**, *63*, 2645.
(13) Kong, H. S.; Glass, J. T.; Davis, R. F. *J. Mater. Res.* **1989**, *1*, 204−214.
(14) Latu-Romain, L.; Chaussende, D.; Chaudouet, P.; Robaut, F.; Berthome, G.; Pons, M.; Madar, R. *J. Cryst. Growth* **2005**, *275*, e609.
(15) Syväjärvi, M.; Sritirawisarn, N.; Yakimova, R. *Mater. Sci. Forum* **2007**, *556−557*, 195.
(16) Markov, I. V. *Crystal growth for beginners; Fundamentals of Nucleation, Crystal Growth and Epitaxy*, 2nd ed.; World Scientific: River Edge, NJ, USA, 2003.
(17) Hirth, J. P.; Pound, G. M. *Condensation and Evaporation: Nucleation and Growth Kinetics*; Pergamon: Oxford, 1963; Chapter B.
(18) Kimoto, T.; Matsunami, H. *J. Appl. Phys.* **1994**, *75*, 850.
(19) Lilov, S. K. *Comput. Mater. Sci.* **1993**, *1*, 363.
(20) Syväjärvi, M.; Yakimova, R.; Tuominen, M.; Kakanakova-Georgieva, A.; MacMillan, M. F.; Henry, A.; Wahab, Q.; Janzen, E. *J. Cryst. Growth* **1999**, *197*, 155.
(21) Yakimova, R.; Syväjärvi, M.; Janzen, E. *Mater. Sci. Forum* **1998**, *264−268*, 159.
(22) Knippenberg, W. F. *Philips Res. Rep.* **1963**, *18*, 161.